Vol. 670: 49–60, 2021 https://doi.org/10.3354/meps13756

MARINE ECOLOGY PROGRESS SERIES Mar Ecol Prog Ser

Published July 22



Incident light on mesophotic corals is constrained by reef topography and colony morphology

Michael P. Lesser^{1,*}, Curtis D. Mobley², John D. Hedley³, Marc Slattery⁴

¹Department of Molecular, Cellular and Biomedical Sciences, and School of Marine Science and Ocean Engineering, University of New Hampshire, Durham, NH 03824, USA

> ²25128 SE 28th Street, Sammamish, WA 98075, USA ³Numerical Optics Ltd, Tiverton EX16 8AA, UK

⁴Department of BioMolecular Science, University of Mississippi, Oxford, MS 38677, USA

ABSTRACT: Mesophotic coral reefs, generally defined as deep reefs between 30 and 150 m, are found worldwide and are largely structured by changes in the underwater light field. Additionally, it is increasingly understood that reef-to-reef variability in topography, combined with quantitative and qualitative changes in the underwater light field with increasing depth, significantly influence the observed changes in coral distribution and abundance. Here, we take a modeling approach to examine the effects of the inherent optical properties of the water column on the irradiance that corals are exposed to along a shallow to mesophotic depth gradient. In particular, the roles of reef topography including horizontal, sloping and vertical substrates are quantified, as well as the differences between mounding, plating and branching colony morphologies. Downwelling irradiance and reef topography interact such that for a water mass of similar optical properties, the irradiance reaching the benthos varies significantly with topography (i.e. substrate angle). Coral morphology, however, is also a factor; model results show that isolated hemispherical colonies consistently 'see' greater incident irradiances across depths, and throughout the day, compared to plating and branching morphologies. These modeled geometric-based differences in the incident irradiances on different coral morphologies are not, however, consistent with actual depth-dependent distributions of these coral morphotypes, where plating morphologies dominate as you go deeper. Other factors, such as the cost of calcification, arguably contribute to these differences, but irradiance-driven patterns are a strong proximate cause for the observed differences in mesophotic communities on sloping versus vertical reef substrates.

KEY WORDS: Mesophotic coral reefs \cdot Optics \cdot Topography \cdot Coral morphology \cdot Light attenuation

Resale or republication not permitted without written consent of the publisher

1. INTRODUCTION

It has been proposed that mesophotic coral reef ecosystems (MCEs) are structured by gradients of abiotic factors such as light and trophic resources (Lesser et al. 2009, 2018), but other factors may also have direct, and indirect, influences on the structure and function of MCEs (Lesser et al. 2018). For instance, the geological history and geomorphology of

modern coral reefs are critical factors that determine the growth, topography and function of MCEs (Locker et al. 2010, Sherman et al. 2010). Changes in geomorphology will also influence the slope of benthic substrates, which is associated with reef-to-reef variability in community composition (Locker et al. 2010, Sherman et al. 2010, Weinstein et al. 2021) and hypothesized to be associated with changes in the irradiances impinging on the reef (Lesser et al. 2018).

As a result, fauna from MCE depths is largely composed of deep-reef specialists including scleractinian corals, demosponges, sclerosponges and soft corals not usually found in shallow waters (Bridge et al. 2012, Slattery & Lesser 2012, 2021, Lesser et al. 2018, Macartney et al. 2020).

1.1. The underwater light environment

The light environment is the primary abiotic factor driving the structure and function of shallow tropical coral reefs (Chalker et al. 1988, Falkowski et al. 1990, Gattuso et al. 2006) and has been hypothesized to significantly influence the ecological structure of most MCE communities as well (Lesser et al. 2009, 2018, 2019). In the optically clear waters of the tropics, the attenuation of photosynthetically available radiation (PAR: 400-700 nm) is modified by the angle of incident light at the surface and the inherent optical properties (IOPs), namely absorption and scattering, of the water column. The absorption coefficient and the volume scattering function, which are dependent on the composition and concentration of dissolved and suspended particulates, are then used in the radiative transfer equation to model underwater irradiances based on depth, time of day and season (Text S1, Fig. S1 in the Supplement at www.int-res. com/articles/suppl/m670p049_supp.pdf). Additionally, the spectral composition of the underwater light field also changes as depth increases, with blue and red wavelengths exhibiting the most significant decreases with increasing depth (Lesser et al. 2009, Eyal et al. 2015). Diffuse attenuation coefficients for downwelling plane irradiance PAR (K_{dPAR}; in units of m⁻¹) have been used to describe the optical characteristics of the water column generally (Kirk 1994, Mobley 1994) and specifically on coral reefs (e.g. Hochberg et al. 2020). These can be used to derive other metrics including the 10% light level, defined as the midpoint of the euphotic zone, and the 1% light level, or the bottom of the euphotic zone where photosynthesis equals respiration, known as the compensation point (Lesser et al. 2009, 2018, Kahng et al. 2010). The K_{dPAR} values from reefs in the Caribbean, Bermuda and the Pacific are variable (Lesser et al. 2018, Hochberg et al. 2020), as are the optical depths calculated for the 1% light level (58-102 m; reviewed in Lesser et al. 2018) and are the result of differences in the IOPs of the water column.

The most commonly used depth-based definitions of MCEs are 30-60~m for upper MCEs and 60-150~m for lower MCEs (Lesser et al. 2018). While the defini-

tion of MCEs based on depth has support (Loya et al. 2016), the strongest correlation in the depth-dependent patterns of mesophotic benthic communities is with the optical properties of the water column, and consequently the resulting variability in irradiances occurring on these benthic environments. (Lesser et al. 2018). In explaining this variability, Lesser et al. (2018) reported a significant difference between high- and low-relief terrestrial environments for coral reefs, with an average (±SD) 1% optical depth of 95 ± 8 m for low-relief associated reefs and 75 \pm 14 m for high-relief or coastal-associated reef systems. As a result, recent studies have suggested defining the depth transitions of MCEs based on the percent of surface PAR occurring where specific community changes have been quantified (Tamir et al. 2019), while others suggest that depth offers no physiological or ecological insights into the variation between the distribution of MCE species or communities (Laverick et al. 2019, 2020) even though most are in general agreement with the current depth-based definitions of MCEs.

However, characterizations based on optics are complicated by the interaction of downwelling plane irradiance (E_d) with the benthos and whether the substrate is horizontal, sloping or vertical in nature (Brakel 1979, Lesser et al. 2018). Brakel (1979) showed that for a specific body of water with known IOPs and sun angle, the plane irradiance PAR (µmol quanta m⁻² s⁻¹) for varyingly sloped substrates revealed that vertical surfaces received ~25% of the PAR measured for horizontal surfaces. Because of the dependence of incident PAR on substrate slope, reef topography can be expected to influence the development of different communities at the same depths in different MCE habitats (Lesser et al. 2018). To further explore the relationship between plane irradiance and substrate slope of the benthos, we undertook an optical analysis to extend the observations described in Lesser et al. (2018) to include varying reef topographies and coral colony morphologies. To reiterate, horizontally infinite water bodies are a onedimensional (1D) radiative transfer problem with depth being the only spatial variable. However, the light field next to a vertical wall originates from the water in front of the wall such that the models needed for understanding and predicting the underwater light field on the varying substrate angles of MCEs, but especially vertical walls, are inherently 3-dimensional (3D). A 3D radiative transfer model, developed for other studies (Mobley & Sundman 2003) was used and incorporated a simple 3D reef wall geometry, the IOPs for clear tropical waters, the incident sky radiance as a function of sun angle, sky conditions, sea surface wave state and the reflectance properties corresponding to photoautotrophic benthic organisms on the wall surface (Lesser et al. 2018). That model was used to simulate irradiances onto an idealized vertical reef oriented in a north–south direction (Lesser et al. 2018). The results of that simulation showed that 1D models are insufficient to describe the underwater light field in the presence of varying sloped substrates. Moreover, 3D models show the inherent effects of the substrate angle on the attenuation of irradiance, and that the amount of PAR available for photoautotrophic organisms can be significantly decreased relative to open water measurements of $E_{\rm d}$ by as much as 50% on a vertical wall (Lesser et al. 2018).

1.2. Functional morphology

As primary photoautotrophs in coral reef ecosystems, the ability of scleractinian corals and their endosymbiotic dinoflagellates (Symbiodiniaceae) to photoacclimatize is inherently linked to their respective ecological success. There is extensive literature on the photobiology of corals, including the absorption and utilization of light as well as the regulation of the photosynthetic apparatus to photoacclimatize under varying irradiances and environmental stressors (Chalker et al. 1983, Dubinsky et al. 1984, Wyman et al. 1987, Lesser et al. 2000, Iglesias-Prieto et al. 2004, Enríquez et al. 2005, Stambler & Dubinsky 2005, Mass et al. 2010, Warner & Suggett 2016). The photobiology of scleractinian corals is often intertwined with the genetics and the specific species of endosymbiotic dinoflagellates (Symbiodiniaceae) harbored by different populations and species of coral (Warner & Suggett 2016, LaJeunesse et al. 2018). A commonly observed outcome of photoacclimatization to low irradiances at the level of the colony for many species of corals is to change their orientation and morphology in an effort to increase the efficiency of their surface area for light capture (Anthony et al. 2005, Todd 2008). Many zooxanthellate scleractinian corals found in MCEs exhibit a fixed plate-like morphology or change shape with depth to a flattened or plate-like morphology as a result of phenotypic plasticity, while corals with fixed mounding and branching morphologies oriented vertically are more common in shallow reef environments (Mass et al. 2007, Hoogenboom et al. 2008, Einbinder et al. 2009, Lesser et al. 2010, Nir et al. 2011, Kramer et al. 2020). Despite these changes, there is a limit to how much changes in morphology can affect rates of photosynthesis and calcification, which have been shown to decline significantly with increasing depth in corals (Mass et al. 2007, Lesser et al. 2010).

Here, we expand the 3D model from Lesser et al. (2018) to include 3 specific reef topologies: a flat back reef, a sloping fringing reef and a vertical fore reef, from shallow to mesophotic depths (see Fig. 1a). We also examine the effects of sloping versus vertical reef substrate into lower mesophotic depths starting at 60 m (see Fig. 1b). We incorporate IOPs directly measured from each reef habitat; these IOPs include the effects of absorption by colored dissolved organic material (CDOM) and suspended particulate material as found on the different reef topologies. We also simulate different 'sensor' shapes representing mounding, plating and branching morphologies of corals. We show that reef topology and coral morphology significantly affect the amount of light incident on corals and discuss this as a proximate cause for the observed changes in the community structure of coral reefs from shallow to mesophotic depths.

2. MATERIALS AND METHODS

The light incident onto the reef was modeled using standard techniques of backward Monte Carlo simulations relative to an idealized reef geometry (Fig. 1). The cardinal orientation of the reef is not part of the run input, but the solar azimuth relative to the reef face is. Here, we model 3 different types of sensors representative of common coral morphologies and provide incident PAR irradiances denoted as PAR_{cos}, PAR_{hs} and PAR_{br} simulating the plating, mounding and branching morphologies of scleractinian corals, respectively, at specific depths (i.e. 10, 12, 20, 30, 40, 50, 58, 65, 75 and 100 m). Specifically, planar irradiance (PAR_{cos}) is the light intercepted per unit area for a plating coral where the plates are orientated parallel to the reef surface. Hemispherical scalar irradiance (PAR_{hs}) is the light incident on an isolated mounding coral per unit area of the reef surface it occupies. PAR_{br} is the average light incident per unit area of the coral surface for branching corals; this can be understood as the average light incident on a polyp in a branching coral. Finally, PAR_o is the spherical quantum scalar irradiance, equivalent to a ' 4π ' sensor just in front of the reef substrate. PAR_o is modeled for reference purposes as it represents what is often measured when studying the photobiology of corals.

In nature, and in a forward Monte Carlo simulation, a light ray is emitted by a source and then traced

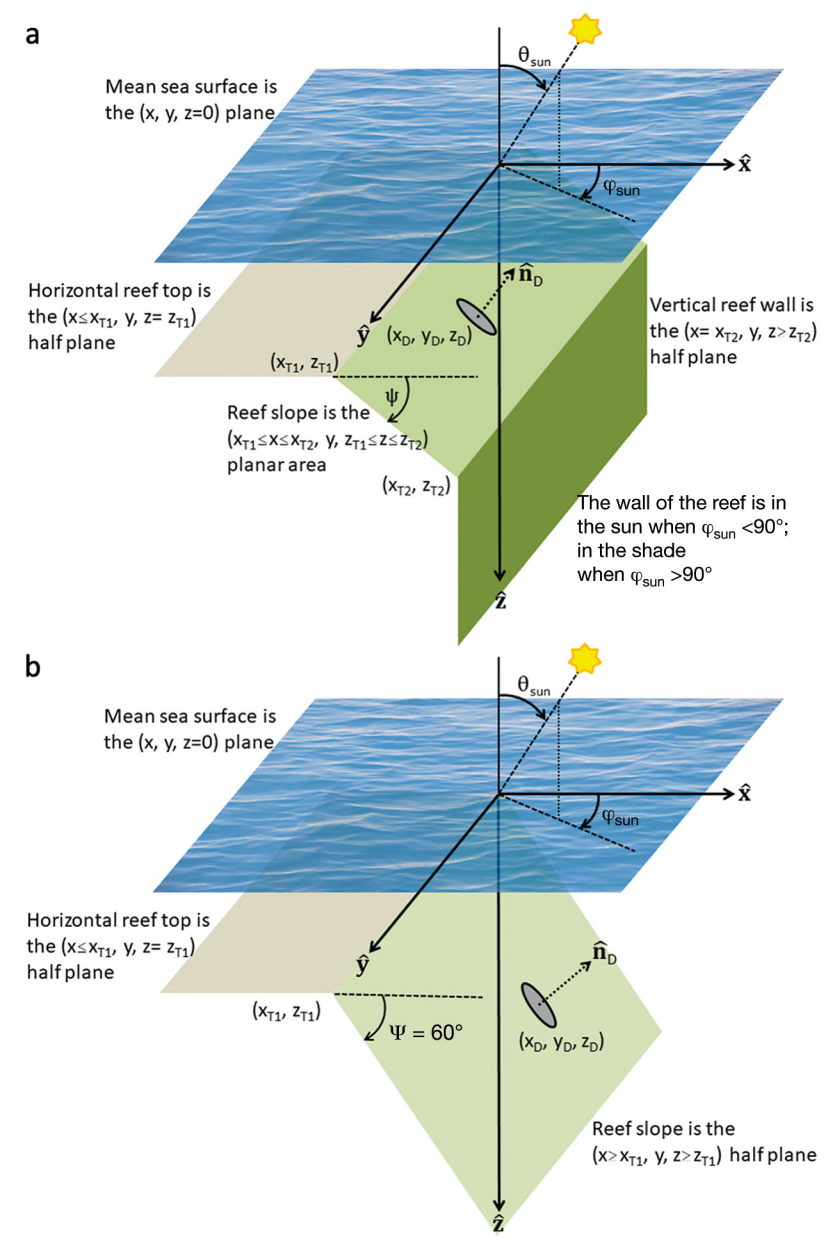


Fig. 1. (a) Coral reef geometry for modeling the underwater light field using ray tracing. The $(\hat{x},\hat{y},\hat{z})$ directions define a coordinate system that defines the sea surface, reef top, reef slope and reef wall with X_{T1} , Z_{T1} and X_{T2} , Z_{T2} representing the top coordinates of the slope and vertical wall respectively. The reef wall faces the + \hat{x} , direction and θ_{sun} is the solar zenith angle. As θ_{sun} increases from 0–90° the sun moves lower in the sky. ϕ_{sun} is the solar azimuthal angle relative to the reef wall. Here, $\phi_{sun}=0^\circ$ corresponds to the sun directly in front of the reef wall; for practical purposes when $\phi_{sun}<90^\circ$ the reef wall will be 'in the sun' and for $\phi_{sun}>90^\circ$ the reef wall is 'in the shade'. The oval at (x_D,y_D,z_D) represents a sensor placed at that location on the surface of the reef slope, whose normal orientation is \hat{n}_D . (b) Same coordinate system for a coral reef with a continuing 60° substrate slope into mesophotic depths versus transitioning to a vertical wall as depicted in (a)

until it reaches a detector (i.e. the coral) or is dropped from further tracking. In the present scenario, the source is the sky, and rays are emitted from different sky directions. Each ray is given the initial weight of

the sky radiance in that direction. The emitted ray is then traced through an arbitrary number of randomly determined interactions with the sea surface and the water column, during which a portion of the initial energy of the ray is absorbed, and the ray's direction changes in accordance with the volume scattering properties of the water column or the angle of incidence onto the wind-blown sea surface. Such calculations, however, are computationally inefficient because most rays never intersect a detector at a given location. The undetected rays are eventually dropped after most of their energy has been absorbed and therefore do not contribute to the estimate of the irradiance reaching the detector. This requires the use of backward Monte Carlo (BMC) simulation as described in detail in Text S1.

This unique 3D radiative transfer problem is then solved ray-by-ray in the BMC simulations. Numerical experience shows that to achieve a statistical estimate of the radiometric quantity of interest that has less than a few percent error due to statistical noise, enough rays must be initialized that the small region of the sky containing the sun receives at least 1000 rays. The number of rays required to achieve this depends on the depth of the detector, the water IOPs, and the radiometric quantity being simulated. For shallow depths, as few as 10⁶ rays must be initialized at each wavelength; for the deepest depths, as many as 1.5×10^8 rays were initialized at each wavelength. The ray-by-ray calculations randomly determined the ray path lengths and directions, along with assessments as to whether the ray has intersected the reef or sea surface. If the ray intersects the reef, the ray is reflected according to the reef reflectance at the point of intersection. If the ray intersects the sea surface,

both transmitted and reflected rays can be generated according to Snell's law and Fresnel's law applied to a sloping wave facet. Additional details of these calculations are provided in Mobley (2018).

The simulation of the branching sensor requires a full directional spectral radiance distribution defined over the sphere of all directions. A method was also developed to generate directional radiance distributions that had the required planar and scalar PAR irradiances (PAR_{cos} and PAR_{hs}), based on modifying radiance distributions from HydroLight (https:// www.numopt.com/hydrolight.html) as described in Text S1. These fully directional radiance distributions also included reflectance from the reef wall in the appropriate hemisphere. The method of generating these distributions, and example plots, are given in Text S1. Briefly, for each location and solar position, the input was the infinite-depth 1D radiance distribution from HydroLight at the same depth with the same IOPs, modified by 2 scalar factors: 's', which uniformly scales the radiance values, and 'w', which introduces a 'wall effect' as a function of the cosine to the vector at right angles to the surface. By this method, radiance distributions for every location and solar theta and azimuth angle were generated.

Given a radiance distribution defined for all directions over the sphere, the 3D model described in Hedley (2008) can be used to determine the light incident on arbitrary shapes embedded in that radiance distribution. Essentially, a surface consisting of polygon facets can be placed like a 'virtual sensor' into the radiance distribution, and the light incident on each facet can be calculated. The surface selfshades but does not affect the input radiance distribution; so in that sense, it is the same process as placing a virtual irradiance sensor in a model such as HydroLight (i.e. the sensor itself is not physically present in the model). In this study, a virtual sensor with a branching morphology was placed into the radiance distributions (Fig. S2). This structure comprised 23520 triangular facets. It was constructed using a parameterized algorithm for generic branching structures; parameters were adjusted until a shape approximating a natural branching coral was obtained. Using the 3D model, the plane PAR irradiance incident on every triangle in the surface is evaluated; this is then summed for all triangles and multiplied by each triangle's area. Finally, dividing by the total triangle area gives the average plane PAR irradiance incident on the coral surface per unit area.

3. RESULTS

Ambient irradiances at the sea surface obtained from the sky model described in Text S1 for tropical latitudes in the summer over the day length period (Fig. 2) are similar to previous, direct, measurements (Brown et al. 1994, Ong et al. 2018) on coral reefs and are an appropriate starting point for the 3D modeling of underwater irradiances. When underwater irradiances are modeled as a 3D problem using the ray tracing approach at a solar zenith angle of 30° (θ_{sun}), the effect of the wall at different solar azimuthal angles relative to the reef wall (ϕ_{sun}) is apparent at shallow depths (Fig. 3) and is greatest for PAR_{cos}. Differences for the sun 'in front of' ($\phi_{sun} = 0$, or sunrise) versus 'behind' (ϕ_{sun} = 180, or sunset) the reef disappear with depth as scattering removes the inherent information about the solar azimuthal and zenith angles. At each depth, the sensor orientation is determined by the reef topography, with the spectral irradiance reflectance of the reef surface (Fig. S1d) determining the fraction of incident irradiance absorbed by the coral at each wavelength, and that the coral absorbs 100% of the incident quanta reaching it integrated across all PAR wavelengths. The remainder is reflected under the assumption that the reef surface is a Lambertian reflector. The model shows that $PAR_o > PAR_{hs} > PAR_{cos} > PAR_{br}$ for all depths and sensor orientations, as expected from purely optical considerations (Fig. 3). For all sensors and depths, the PAR values absorbed by each sensor type can be seen to vary over the day in a qualitatively similar manner, with the magnitudes depending strongly on the depth, reef orientation and water IOPs. (Fig. 3). These values are for the specific reef topography that includes a vertical wall at depths greater than 60 m (Fig. 1a). It is important to note that for each depth the attenuation of irradiance is determined by one specific set of IOPs used from the sea surface to that depth (i.e. a model run for the sensor on the wall at 75 m uses the fore reef IOPs from the

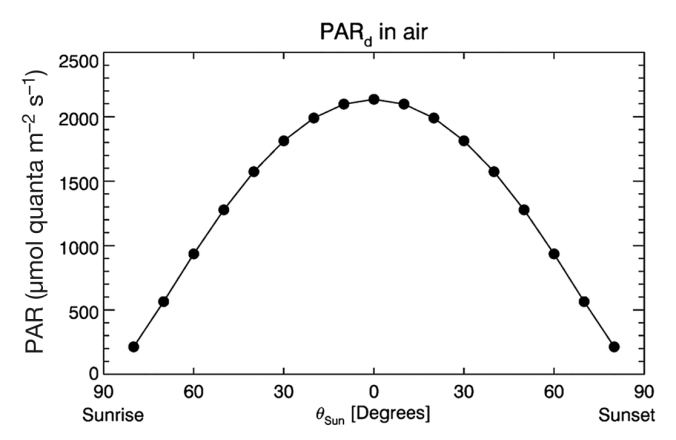


Fig. 2. Plot of downwelling photosynthetically active radiation (PAR_d) in air for $\phi_{sun}=0^{\circ}$ relative to the reef wall from a 1D HydroLight output as θ_{sun} traverses the sky from sunrise to sunset

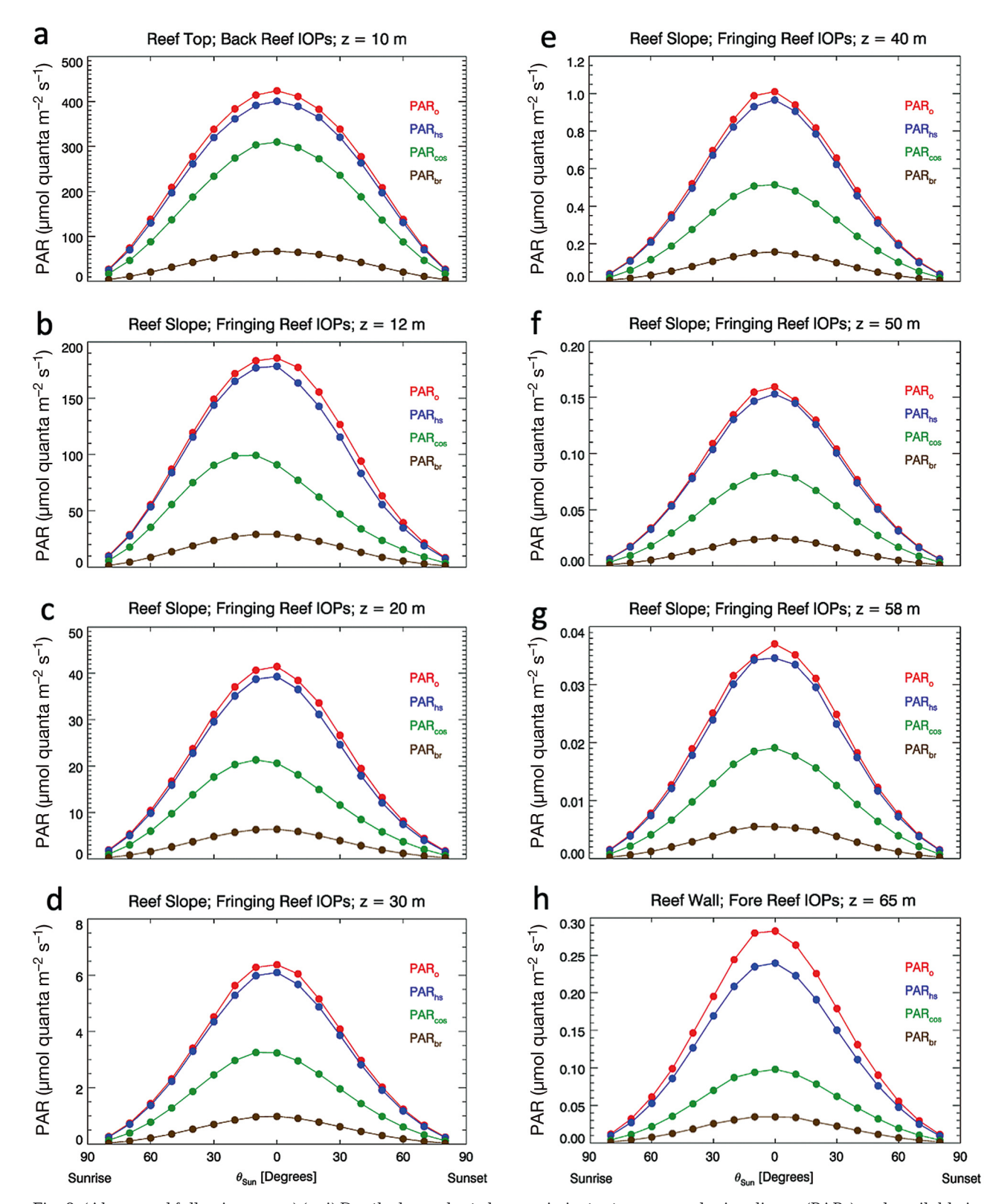
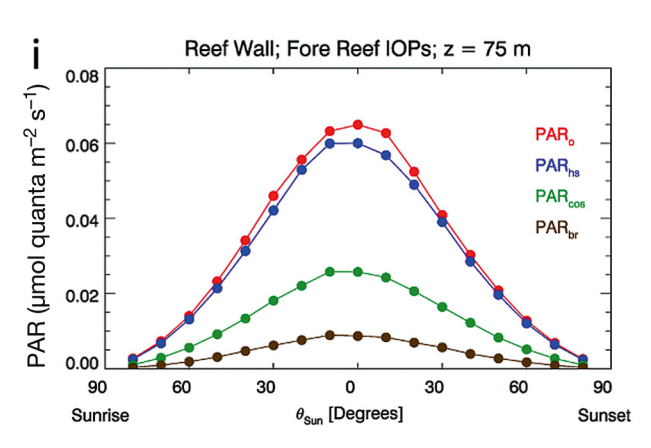


Fig. 3. (Above and following page.) (a–j) Depth-dependent changes in instantaneous scalar irradiance (PAR $_{o}$) and available irradiance for hemispherical (PAR $_{hs}$), cosine (PAR $_{cos}$) and branching (PAR $_{br}$) sensors from the ray tracing simulations assuming 100% absorption of all available quanta. The sunrise side of the plot corresponds to $\phi_{sun}=0^{\circ}$ and sunset to $\phi_{sun}=180^{\circ}$, as θ_{sun} traverses the sky from sunrise to sunset for a shallow to mesophotic depth gradient that includes a vertical wall beginning at ~60 m. IOPs: inherent optical properties



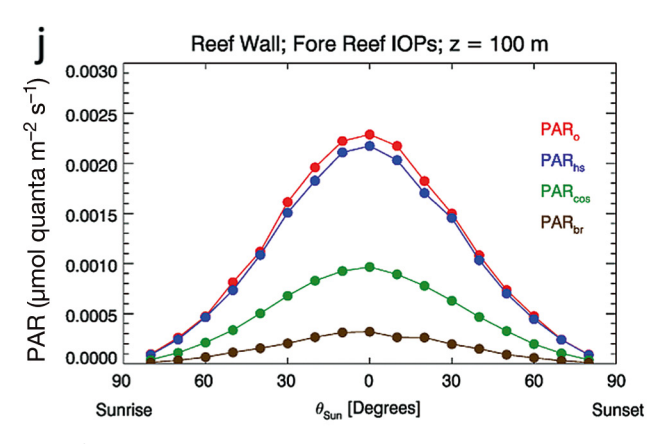


Fig. 3. (continued)

sea surface down to 75 m). The current BMC model does not allow for depth-dependent changes in IOPs within a single simulation run. Therefore, at 65, 75 and 100 m (Fig. 3h,i,j, respectively) the changes in irradiance observed are a function of not only the fore reef IOPs, with their lower attenuation of PAR, but the changes in reef topography and sensor orientation which clearly results in lower incident PAR absorbances for the PAR $_{\rm cos}$ and PAR $_{\rm br}$ sensors, especially compared to the PAR $_{\rm hs}$ sensor at 75 and 100 m (Fig. 3i,j, respectively).

If we then look specifically at the effect of substrate angle by extending our 60° fringing reef slope onto the fore reef out to ~100 m, we observe an increase in PAR at 65, 75 and ~100 m of 26, 40 and 62%, respectively (Fig. 4a–c). There is also an increase in the PAR absorbed for all sensor types on a sloping substrate compared to values from the model runs where a vertical wall occurs beyond ~60 m (Fig. 4d–f), with the largest increases observed for the PAR_{cos} sensor and the lowest increases for the PAR_{br} sensor (Fig. 4d–f).

4. DISCUSSION

In the wider Caribbean basin, the Red Sea and Indo-Pacific, the distribution of all scleractinian coral morphotypes shows a general decline in percent cover with depth (but see Kramer et al. 2020 for an exception in the Red Sea), but a relatively greater abundance of platelike corals at mesophotic depths followed by mounding morphs and the near absence of branching coral species (Goreau & Wells 1967, Goreau & Goreau 1973, Kühlmann 1983, Fricke & Meischner 1985, Liddell & Ohlhorst 1987, 1988, Liddell et al. 1997, Kahng et al. 2010, Bridge et al. 2012, Hoeksema et al. 2017, Kramer et al. 2020). Addition-

ally, early studies specifically identified community breaks in coral communities between the upper and lower mesophotic zones at ~50–60 m depth (Liddell & Ohlhorst 1987, 1988, Liddell et al. 1997) which have been further supported by a meta-analysis of coral reef community structure from shallow to mesophotic depths (Lesser et al. 2019).

Many of these studies suggested that the attenuation of solar irradiance, and the transition from photoautotrophy to heterotrophy, is the most important factor regulating the observed patterns of zonation from shallow to mesophotic depths, especially for the scleractinian corals of the community (see Lesser et al. 2018). Our results show that sloping substrates receive more incident light than vertical substrates. If the productivity and growth of corals on sloping substrates increases proportional to that increase in incident irradiances, it would be predicted that corals would increase their benthic cover with increasing depth compared to vertical substrates. If we look at published studies on MCEs with shallow sloping substrates (25-45°), we see the development of deep buttresses down to 65 m depth and significant coral populations in the mesophotic from 47-70 m averaging ~13% benthic cover, with the greatest cover of ~28% at 70 m depth in Puerto Rico (Sherman et al. 2010). In contrast, coral cover in the Bahamas along a vertical wall (>70°) in the mesophotic zone from 46-91 m averages ~7% and showed only 2% coral cover at 76 m (Slattery & Lesser 2012). More recent studies have included broader spatial and temporal coverage of irradiance measurements used to define community transitions along the shallow to mesophotic depth gradient based on the attenuation of light as opposed to depth per se (Tamir et al. 2019, Laverick et al. 2020). While generally supportive of current depth definitions for upper and lower mesophotic depth boundaries, these studies, and

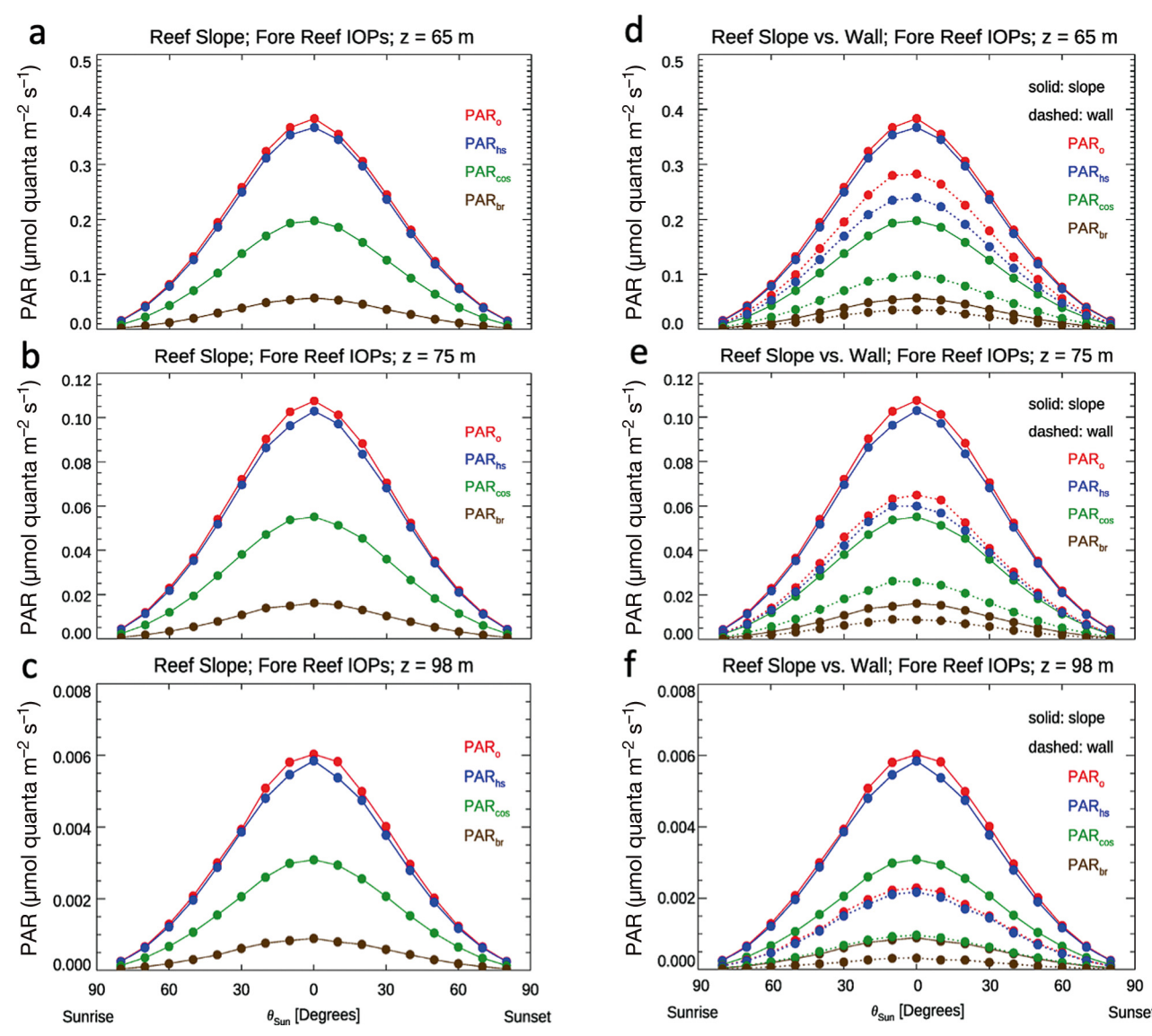


Fig. 4. (a–c) Depth-dependent changes in instantaneous scalar irradiance (PAR $_{o}$) and available irradiance for hemispherical (PAR $_{hs}$), cosine (PAR $_{cos}$) and branching (PAR $_{br}$) sensors (corresponding to the different morphologies) from the ray tracing simulations assuming 100% absorption of all available quanta and a $\phi_{sun}=0^{\circ}$ or $\phi_{sun}=180^{\circ}$, as θ_{sun} traverses the sky from sunrise to sunset for a shallow to mesophotic depth gradient that includes a vertical wall beginning at ~60 m. (d–f) Comparison of changes in PAR $_{o}$ and available irradiance for PAR $_{hs}$, PAR $_{cos}$ and PAR $_{br}$ sensors for 65, 75 and ~100 m model outputs for vertical (dashed lines) and sloping (solid lines). IOPs: inherent optical properties

previous works (see Lesser et al. 2018 for review), do not explicitly examine what individual corals on a reef actually 'see' at any depth as it relates to light. However, Laverick et al. (2019), studying the plating coral *Agaricia lamarki* from shallow (<30 m) to upper mesophotic (30–60 m) depths in the Caribbean, suggested that coral samples from both shallow and upper mesophotic depths were physiologically similar because of similar irradiance microhabitats, making depth an inappropriate proxy to ecologically characterize coral populations from discrete depths. However, in a study on the mounding coral *Montas*-

traea cavernosa, Lesser et al. (2010) found that corals from shallow and upper mesophotic depths were also physiologically similar in many respects and that multiple physiological characteristics, including primary productivity, did not differ significantly in a depth-dependent manner until the lower mesophotic zone (60–150 m).

In the present study, we used a radiative transfer approach that includes BMC ray tracing combined with measured inherent optical properties of the water column. While BMC ray tracing has been used previously to describe irradiances on shallow (~5 m)

corals of different morphologies and pigmentation (Ong et al. 2018), their output was broadband red, green and blue (RGB) values, which were then converted to luminance, a metric based on the spectral response of the human eye, and to energetic units (W m^{-2}) using a conversion factor that is ~25 % lower than previous studies have recommended (e.g. Morel & Smith 1974). The approach described here represents a significant advancement via the application of backward ray tracing to compute the incident irradiance upon individual corals of different morphologies over the day, and as a function of reef topography and depth. An unambiguous hierarchy of coral morphologies clearly shows that the irradiance seen by corals declines from mounding to plating to branching corals, regardless of reef topography, while reef topography has additional, and significant, effects on those irradiances. Increased ability to capture light, and its potential for an increase in productivity, are also associated with morphological changes in corals such as branch flattening (Einbinder et al. 2009), the transition from mounding to plating (Lesser et al. 2010) and the general increase in coral species with plating morphology (e.g. agariciid corals) at mesophotic depths (Kahng et al. 2019, Padilla-Gamiño et al. 2019). Changes in photophysiological performance of plating morphologies is also consistent with optical models that have examined the role of morphology in the protection of shallow corals from photoinhibition, and where colonies flatten to increase their efficiency of light capture under low irradiances in order to maintain positive rates of photosynthesis (Anthony et al. 2005, Hoogenboom et al. 2008).

For coral reef environments, the underwater light environment is the critical abiotic factor driving the zonation patterns of scleractinian corals generally, and MCEs in particular (Lesser et al. 2009, 2018). Our previous simulations (Lesser et al. 2018), and those presented here, underscore the fact that E_d measured in the water column is not what corals on substrates of varying angles (i.e. vertical versus sloping) are exposed to, and that colony morphology and reef topography have the potential to significantly affect both coral productivity and growth. Importantly, mounding corals a priori have better bio-optical characteristics and experience greater incident irradiances at all sun and substrate angles. However, this primarily applies to isolated mounding corals where the sides have a 'free view' of incident light; when found aggregated together, mounding corals would increasingly intercept the same light per unit area of the reef as a plating coral. Additionally, the gradient from a hemispherical to a plating coral represents a

potential decrease in total light capture per unit reef area. That is, the coral surface area is increased in a hemispherical colony with the same radius as a plating colony; a planar coral of radius r has a surface area of πr^2 , whereas a hemispherical coral of radius r has a surface area of $2\pi r^2$, but under a diffuse radiance distribution each point on the surface of the colony experiences the same irradiance. As a result, the hemispherical coral always captures more light than a plating coral per unit area of the reef. A branching colony structure is a continuation of this gradient; it has more surface area for the same area of reef, and the efficiency of light capture would increase proportionately were it not for self-shading (Fig. S2). Branching morphologies therefore always capture less light per unit area of the coral surface compared to the other morphologies because of selfshading and only become a successful light capture strategy when there are saturating light conditions throughout the day (i.e. shallow water) to maintain photosynthesis despite self-shading. In contrast, a hemispherical colony does not shade itself and therefore, when isolated and under diffuse light, maintains the highest polyp-level irradiances and potential productivity under a broad range of irradiances. How much of this productivity potential translates into growth? Mounding corals consistently grow more slowly and have lower skeletal densities than plating or branching corals (Hughes 1987, Swain et al. 2018). For mounding corals, skeletal density does increase with depth but is always lower than the values observed in plating corals at any depth (Hughes 1987). However, energetic costs for mounding corals are higher overall because of the increase in calcified biomass associated with their significantly lower surface area to volume ratios compared to plating corals (Madin et al. 2016). Because of these inherently higher energetic costs for calcification in mounding corals, and since productivity potential is light-dependent, the advantage for mounding corals over plating corals decreases as depth increases.

Our results do not *a priori* explain the phenotypic plasticity observed for morphology from hemispherical to plating morphology with increasing depth (e.g. Lesser et al. 2010), the transition of vertically oriented plates to flattened plates in agaricids (Anthony et al. 2005, Hoogenboom et al. 2008) or the endemism of many coral species in the lower mesophotic with plating morphology (e.g. Padilla-Gamiño et al. 2019). One possible explanation is to consider the polyp-scale requirements to maintain net positive photosynthesis. A given surface intercepts light most efficiently when it is at right angles to the direction

from which the light is incident. Therefore, the most efficient location for coral tissue containing algal symbionts is on a horizontal surface to maximally intercept downwelling irradiance, which would explain the dominance of plating corals on horizontal substrates on many lower MCEs (e.g. Padilla-Gamiño et al. 2019). In this study, plating corals were assumed orientated parallel to the reef surface, and while many plating corals can extend horizontally from the reef wall in the upper mesophotic zone (30–60 m), in the lower mesophotic zone (60–150 m) they are often oriented parallel with the reef as sedimentation and substrate stability as sources of disturbance increase in importance and prevent coral growth in a horizontal plane (Sheppard 1982).

The differences in incident irradiances upon the different coral morphologies reported here, and their interaction with reef topography, did not consider the ultimate fate of each quanta and the effects of smallscale optics in the tissues and skeleton of different coral morphologies (Enríquez et al. 2005, 2017, Kahng et al. 2012, Wangpraseurt et al. 2012), depthdependent changes, and endemism, in the community composition of the photoautotrophic endosymbiont (Symbiodiniaceae) of mesophotic corals (Lesser et al. 2010, Bongaerts et al. 2015, Pochon et al. 2015, Ziegler et al. 2015), the ability to photoacclimatize to extremely low irradiances (Einbinder et al. 2016, Padilla-Gamiño et al. 2019) or the availability and stoichiometry of dissolved inorganic nutrients (Ferrier-Pagès et al. 2000). Of these factors, the effect that provides the most probable explanation for the difference in the functional performance of an ideal versus a real sensor (i.e. coral) is the light scattering properties of the coral skeleton. It has been shown that for corals, both the tissues and skeleton interact with light to produce multiple scattering events which increase the pathlength, and therefore absorption, of individual quanta by the reaction centers of the symbiotic Symbiodiniaceae for photochemistry (Kühl et al. 1995, Enríquez et al. 2005, 2017, Wangpraseurt et al. 2012). Depending on the skeletal microstructure, there is a corresponding 'amplification' factor which leads to increases in light absorption and improved photosynthetic performance, especially in low irradiance environments, that improves further when combined with unique photosynthetic characteristics of Symbiodiniaceae in mesophotic corals (e.g. Einbinder et al. 2016). The coral skeletal morphology is the significant contributor to the variability of this amplification phenomenon where typically mounding corals exhibit the lowest scattering and plating corals the highest. In fact, using a metric of integrated scattering over the entire coral skeleton called the 'light enhancement factor' (LEF), Enríquez et al. (2017) showed that plating coral species had significantly higher LEF values of as much as ~25%, a clear advantage at mesophotic depths compared to massive coral species. This advantage can be seen in the Red Sea where mounding and plating corals have an inverse relationship with depth, such that mounding corals are dominant down to 40 m and plating corals dominant thereafter with 100% cover at 100 m (Kramer et al. 2020). This strongly suggests that the skeletal architecture, and the amount of scattering it produces, could overcome geometric constraints (e.g. Enríquez et al. 2017).

As suggested by Laverick et al. (2017), coral species assemblage may be a good indicator for deviations from the commonly used depth-dependent definitions between shallow, upper mesophotic and lower mesophotic reef zones. These deviations are, however, the result of the irradiance 'seen' by individual corals, the influences of their respective morphology and the type and topography of their habitat. Contraction of these ecological zones or the presence of endemic mesophotic corals in shallow habitats such as lagoons with decreased water transparency (Colin & Lindfield 2019, Laverick et al. 2020) provide evidence for the strong influence on the ecological zonation of scleractinian corals caused by the variability in irradiance. The general relationship between irradiance and the ecological distribution of coral species observed on most, but not all, MCEs still supports the broad use of the depth-dependent definition between upper and lower mesophotic communities at ~60 m (Lesser et al. 2019) unless reef-specific differences in the underwater light field, and patterns of ecological zonation, are quantified. Additionally, by characterizing the underwater irradiance field at the level of the coral colony associated with changes in reef topography and morphology, we provide a framework for ecological descriptions, and hypothesis testing, on the functional attributes of not only corals but other photoautotrophs (e.g. macrophytes) on MCEs.

Acknowledgements. Support for this research was provided by NSF Biological Oceanography grant nos. OCE-1632348 and -1632333 to M.P.L. and M.S., respectively. We thank Brandon Russell and Heidi Dierssen for providing their measured IOP data for use in the Monte Carlo simulations.

LITERATURE CITED

Anthony KRN, Hoogenboom MO, Connolly SR (2005) Adaptive variation in coral geometry and the optimization of internal colony light climates. Funct Ecol 19:17–26

- Bongaerts P, Frade PR, Hay KB, Englebert N and others (2015) Deep down on a Caribbean reef: lower mesophotic depths harbor a specialized coral-endosymbiont community. Sci Rep 5:7652
 - Brakel WH (1979) Small-scale spatial variation in light available to coral reef benthos: quantum irradiance measurements from a Jamaican reef. Bull Mar Sci 29:406–413
- Bridge TCL, Fabricius KE, Bongaerts P, Wallace CC, Muir PR, Done TJ, Webster JM (2012) Diversity of Scleractinia and Octocorallia in the mesophotic zone of the Great Barrier Reef, Australia. Coral Reefs 31:179–189
- Brown BE, Dunne RP, Scoffin TP, Le Tessier MDA (1994) Solar damage in intertidal corals. Mar Ecol Prog Ser 105: 219–230
- *Chalker BE, Dunlap WC, Oliver JK (1983) Bathymetric adaptations of reef-building corals at Davies Reef, Great Barrier Reef, Australia. II. Light saturation curves for photosynthesis and respiration. J Exp Mar Biol Ecol 73: 37–56
- Chalker BE, Barnes DJ, Dunlap WC, Jokiel PL (1988) Light and reef-building corals. Interdiscip Sci Rev 13:222–237
 - Colin PL, Lindfield SJ (2019) Palau. In: Loya Y, Puglise K, Bridge T (eds) Mesophotic coral ecosystems. Coral reefs of the world. Springer International, Cham, p 285–299
- Dubinsky Z, Falkowski PG, Porter JW, Muscatine L (1984)
 Absorption and utilization of radiant energy by lightand shade-adapted colonies of the hermatypic coral
 Stylophora pistillata. Proc R Soc B 222:203–214
- Einbinder S, Mass T, Brokovich E, Dubinsky Z, Erez J, Tchernov D (2009) Changes in morphology and diet of the coral *Stylophora pistillata* along a depth gradient. Mar Ecol Prog Ser 381:167–174
- Einbinder S, Gruber DF, Salomon E, Liran O, Keren N, Tchernov D (2016) Novel adaptive photosynthetic characteristics of mesophotic symbiotic microalgae within the reefbuilding coral, *Stylophota pistillata*. Front Mar Sci 3:195
- Enríquez S, Méndez ER, Iglesias-Prieto R (2005) Multiple scattering on coral skeletons enhances light absorption by symbiotic algae. Limnol Oceanogr 50:1025–1032
- Enríquez S, Méndez ER, Hoegh-Guldberg O, Iglesias-Prieto R (2017) Key functional role of the optical properties of coral skeletons in coral ecology and evolution. Proc R Soc B 284:20161667
- Eyal G, Wiedenmann J, Grinblat M, D'Angelo C and others (2015) Spectral diversity and regulation of coral fluorescence in a mesophotic reef habitat in the Red Sea. PLOS ONE 10:e0128697
 - Falkowski PG, Jokiel PL, Kinzie RA III (1990) Irradiance and corals. In: Dubinsky Z (ed) Coral reefs. Ecosystems of the world. Elsevier, Amsterdam, p 89–107
- Ferrier-Pagès C, Gattuso JP, Dallot S, Jaubert J (2000) Effect of nutrient enrichment on growth and photosynthesis of the zooxanthellate coral *Stylophora pistillata*. Coral Reefs 19:103–113
- Fricke H, Meischner D (1985) Depth limits of Bermudan scleractinian corals: a submersible study. Mar Biol 88: 175–187
- Gattuso JP, Gentilli B, Duarte CM, Kleypas JA, Middleburg JJ, Antoine D (2006) Light availability in the coastal ocean: impact on the distribution of benthic photosynthetic organisms and their contribution to primary production. Biogeosciences 3:489–513
 - Goreau TF, Goreau NI (1973) The ecology of Jamaican coral reefs. II. Geomorphology, zonation and sedimentary phases. Bull Mar Sci 23:399–464

- Goreau TF, Wells JW (1967) The shallow-water Scleractinia of Jamaica: revised list of species and their vertical distribution range. Bull Mar Sci 17:442–453
- Hedley J (2008) A three-dimensional radiative transfer model for shallow reef environments. Opt Express 16: 21887–21902
- *Hochberg EJ, Peltier SA, Maritorena S (2020) Trends and variability in spectral diffuse attenuation of coral reef waters. Coral Reefs 39:1377–1389
- Hoeksema B, Bongaerts P, Baldwin CC (2017) High coral cover at lower mesophotic depths: a dense *Agaricia* community at the leeward side of Curacao, Dutch Caribbean. Mar Biodivers 47:67–70
- Hoogenboom MO, Connolly SR, Anthony KRN (2008) Interactions between morphological and physiological plasticity optimize energy acquisition in corals. Ecology 89: 1144-1154
- *Hughes TP (1987) Skeletal density and growth form of corals. Mar Ecol Prog Ser 35:259–266
- Iglesias-Prieto R, Beltrán VH, LaJeunesse TC, Reyes-Bonilla H, Thomé PE (2004) Different algal symbionts explain the vertical distribution of dominant reef corals in the eastern Pacific. Proc R Soc B 271:1757–1763
- *Kahng SE, Garcia-Sais JR, Spalding HL, Brokovich E and others (2010) Community ecology of mesophotic coral reef ecosystems. Coral Reefs 29:255–275
- Kahng SE, Hochberg EJ, Apprill A, Wagner D, Luck DG, Perez D, Bidigare RR (2012) Efficient light harvesting in deep-water zooxanthellate corals. Mar Ecol Prog Ser 455:65–77
 - Kahng SE, Akkaynak D, Shlesinger T, Hochberg EJ, Wiedenmann J, Tamir R, Tchernov D (2019) Light, temperature, photosynthesis, heterotrophy, and the lower depth limits of mesophotic coral ecosystems. In: Loya Y, Puglise KA, Bridge T (eds) Mesophotic coral ecosystems. Coral reefs of the world. Springer International, Cham, p 801–828
 - Kirk JTO (1994) Light and photosynthesis in aquatic ecosystems, 2nd edn. Cambridge University Press, Cambridge
- Kramer N, Tamir R, Eyal G, Loya Y (2020) Coral morphology portrays the spatial distribution and population sizestructure along a 5–100 m depth gradient. Front Mar Sci 7:615
- Kühl M, Cohenm Y, Dalsgaardm T, Jørgensen BB, Revsbech NP (1995) Microenvironment and photosynthesis of zooxanthellae in scleractinian corals studied with microsensors for O₂, pH and light. Mar Ecol Prog Ser 117:159–172
- → Kühlmann DHH (1983) Composition and ecology of deep-water coral association. Helgol Meeresunters 36: 183–204
- LaJeunesse TC, Parkinson JE, Gabrielson PW, Jeong HJ, Reimer JD, Voolstra CR, Santos SR (2018) Systematic revision of Symbiodiniaceae highlights the antiquity and diversity of coral endosymbionts. Curr Biol 28:2570–2580
- Laverick JH, Andradi-Brown DA, Rogers AD (2017) Using light-dependent Scleractinia to define the upper boundary of mesophotic coral ecosystems on the reefs of Utila, Honduras. PLOS ONE 12:e0183075
- *Laverick JH, Green TK, Burdett HL, Newton J, Rogers AD (2019) Depth alone is an inappropriate proxy for physiological change in the mesophotic coral *Agaraici lamarki*. J Mar Biol Assoc UK 99:1535–1546
- Laverick JH, Tamir R, Eyal G, Loya Y (2020) A generalized light-driven model of community transitions along coral reef depth gradients. Glob Ecol Biogeogr 29:1554–1564

- Lesser MP, Mazel C, Phinney D, Yentsch CS (2000) Light 🧩 Nir O, Gruber DF, Einbinder S, Kark S, Tchernov D (2011) absorption and utilization by colonies of the congeneric hermatypic corals Montastraea faveolata and Montastraea cavernosa. Limnol Oceanogr 45:76-86
- Lesser MP, Slattery M, Leichter JJ (2009) Ecology of mesophotic coral reefs. J Exp Mar Biol Ecol 375:1-8
- 减 Lesser MP, Slattery M, Stat M, Ojimi M, Gates RD, Grottoli A (2010) Photoacclimatization by the coral Montastraea cavernosa in the mesophotic zone: light, food, and genetics. Ecology 91:990-1003
- Lesser MP, Slattery M, Mobley CD (2018) Biodiversity and functional ecology of mesophotic coral reefs. Annu Rev Ecol Syst 49:49-71
- Lesser MP, Slattery M, Laverick JH, Macartney KJ, Bridge T (2019) Global community breaks at 60 m on mesophotic coral reefs. Glob Ecol Biogeogr 28:1403-1416
 - Liddell WD, Ohlhorst SL (1987) Patterns of reef community structure, North Jamaica. Bull Mar Sci 40:311-329
- Liddell WD, Ohlhorst SL (1988) Hard substrata community patterns, 1-120 m, North Jamaica. Palaios 3:413-423
 - Liddell WD, Avery WE, Ohlhorst SL (1997) Patterns of benthic community structure, 10-250 m, the Bahamas. Proc 8th Int Coral Reef Symp, Panama City 1:437–442
- 🔭 Locker SD, Armstrong RA, Battista TA, Rooney JJ, Sherman C, Zawada DG (2010) Geomorphology of mesophotic coral ecosystems: current perspectives on morphology, distribution, and mapping strategies. Coral Reefs 29: 329 - 345
- Loya Y, Eyal G, Trebitz T, Lesser MP, Appeldoorn R (2016) Theme section on mesophotic coral ecosystems: advances in knowledge and future perspectives. Coral
- Macartney KJ, Pankey MS, Slattery M, Lesser MP (2020) Trophodynamics of the sclerosponge Ceratoporella nicholsoni along a shallow to mesophotic depth gradient. Coral Reefs 39:1829-1839
- Madin JS, Hoogenboom MO, Connolly SR, Darling ES and others (2016) A trait-based approach to advance coral reef science. Trends Ecol Evol 31:419-428
- Mass T, Einbinder S, Brokovich E, Shashar N, Vago R, Erez J, Dubinsky Z (2007) Photoacclimation of Stylophora pistillata to light extremes: metabolism and calcification. Mar Ecol Prog Ser 334:93-102
- Mass T, Kline DI, Roopin M, Veal CJ, Cohen S, Lluz D, Levy O (2010) The spectral quality of light is a key driver of photosynthesis and photoadaptation in Stylophora pistillata colonies from different depths in the Red Sea. J Exp Biol 213:4084-4091
 - Mobley CD (1994) Light and water. Radiative transfer in natural waters. Academic Press, New York, NY
 - Mobley CD (2018) Monte Carlo ray tracing for coral reeflight calculations. www.oceanopticsbook.info/view/ references/publications
 - Mobley CD, Sundman LK (2003) Effects of optically shallow bottoms on upwelling radiances: inhomogeneous and sloping bottoms. Limnol Oceanogr 48:239-336
- Morel A, Smith RC (1974) Relation between total quanta and total energy for aquatic photosynthesis. Limnol Oceanogr 19:591-600

Editorial responsibility: Chris Langdon, Coral Gables, Florida, USA Reviewed by: R. Tamir and 2 anonymous referees

- Changes in scleractinian coral Seriotopora hystrix morphology and its endocellular Symbiodinium characteristics along a bathymetric gradient from shallow to mesophotic reef. Coral Reefs 30:1089-1100
- Ong RH, King AJC, Caley MJ, Mullins BJ (2018) Prediction of solar irradiance using ray-tracing techniques for coral macro- and micro-habitats. Mar Environ Res 141:75-87
- 🏋 Padilla-Gamiño JL, Roth MS, Rodrigues LJ, Bradley CJ and others (2019) Ecophysiology of mesophotic reef-building corals in Hawai'i is influenced by symbiont-host associations, photoacclimatization, trophic plasticity, and adaptation. Limnol Oceanogr 64:1980-1995
- Pochon X, Forsman ZH, Spalding HL, Padilla-Gamiño JL, Smith CM, Gates RD (2015) Depth specialization in mesophotic corals (Leptoseris spp.) and associated algal symbionts in Hawai'i. R Soc Open Sci 2:140351
- Sheppard CRC (1982) Coral populations on reef slopes and their major controls. Mar Ecol Prog Ser 7:83-115
- Sherman C, Nemeth M, Ruíz H, Bejarano I and others (2010) Geomorphology and benthic cover of mesophotic coral ecosystems of the upper insular slope of southwest Puerto Rico. Coral Reefs 29:347-360
 - Slattery M, Lesser MP (2012) Mesophotic coral reefs: a global model of community structure and function. Proc 12th Intl Coral Reef Symp, Cairns 1:9-13
- Slattery M, Lesser MP (2021) Gorgonians are foundation species on sponge-dominated mesophotic coral reefs in the Caribbean. Front Mar Sci 8:654268
- Stambler N, Dubinsky Z (2005) Corals as light collectors: an integrating sphere approach. Coral Reefs 24:1-9
- Swain TD, Lax S, Lake N, Grooms H, Backman V, Marcellino LA (2018) Relating coral skeletal structures at different length scales to growth, light availability to Symbiodinium, and thermal bleaching. Front Mar Sci 5:450
- Tamir R, Eyal G, Kramer N, Laverick JH, Loya Y (2019) Light environment drives the shallow-to-mesophotic coral community transition. Ecosphere 10:e02839
- Todd PA (2008) Morphological plasticity in scleractinian corals. Biol Rev Camb Philos Soc 83:315-337
- XWangpraseurt D, Larkum AWD, Ralph PJ, Kühl M (2012) Light gradients and optical microniches in coral tissues. Front Microbiol 3:316
 - Warner ME, Suggett DJ (2016) The photobiology of Symbiodinium spp. linking physiological diversity to the implications of stress and resilience. In: Goffredo S, Dubinsky Z (eds) The Cnidaria: past, present and future. Springer International, Cham, p 489-509
- Weinstein DK, Tamir R, Kramer N, Eyal G and others (2021) Mesophotic reef geomorphology categorization, habitat identification, and relationships with surface cover and terrace formation in the Gulf of Agaba. Geomorphology
- *Wyman KD, Dubinsky Z, Porter JW, Falkowski PG (1987) Light absorption and utilization among hermatypic corals: a study in Jamaica, West Indies. Mar Biol 96:283-292
- Ziegler M, Roder CM, Büchel C, Voolstra CR (2015) Mesophotic coral depth acclimatization is a function of host-specific symbiont physiology. Front Mar Sci 2:4

Submitted: March 29, 2021 Accepted: May 17, 2021

Proofs received from author(s): July 15, 2021